


Lingyun Zhang^{1,2}, Yazeng Gao^{1,2}, Shuaiqiang Ming¹, Weier Lu^{1,2,3}  and Yang Xia^{1,2,4,5}

Research Article

Cite this article: Zhang L, Gao Y, Ming S, Lu W, Xia Y (2024) Numerical analysis of X-ray multilayer Fresnel zone plates with high aspect ratios. *Laser and Particle Beams* **42**, e3, 1–6. <https://doi.org/10.1017/lpb.2024.3>

Received: 2 November 2023

Revised: 17 April 2024

Accepted: 24 April 2024

Keywords:

atomic layer deposition; coupled wave theory; diffraction efficiency; high aspect ratio; multilayer Fresnel zones plates; numerical analysis; X-ray optics

Corresponding author: Weier Lu;Email: luweier@ime.ac.cn

¹Institute of Microelectronics of the Chinese Academy of Sciences, Beijing, People's Republic of China; ²University of Chinese Academy of Sciences, Beijing, People's Republic of China; ³Key Laboratory of Science and Technology on Silicon Devices, Chinese Academy of Sciences, Beijing People's Republic of China; ⁴University of Science and Technology of China, Hefei, People's Republic of China and ⁵Suzhou Institute for Advanced Research, University of Science and Technology of China, Suzhou, People's Republic of China

Abstract

A partition calculation method (PCM) for calculating the diffraction efficiency of multilayer Fresnel zone plate with high aspect ratio is proposed. In contrast to the traditional theory, PCM designs and evaluates Fresnel zone plate (FZP) considering material pairs, all zone widths, thicknesses and X-ray energy more completely. The results obtained through PCM are validated by comparing them with the complex amplitude superposition theory and coupled wave theory numerical results. The PCM satisfies the requirements of the theoretical investigation of FZP with small outermost zone width (dr_N) and large thickness (t). Combining proper numerical analysis with the experimental conditions will present a great potential to break through the imaging performance of X-ray microscopy.

Introduction

X-ray microscopy is a powerful technique to observe the internal structure of an object nondestructively with the spatial resolution in submicron or nanoscale, which has been widely applied in industrial and scientific research fields (Refs 1–4). Fresnel zone plate (FZP) is a typically utilized diffractive optics to realize the high resolution in X-ray microscopy (Refs 5–8). It consists of a set of coaxial rings with radially decreasing zone widths from inner to outside depending on the zone plate law. The concentric rings or the zones are generally made up of two types of materials that are alternating opaque and transparent for the incident X-ray. The diffraction efficiency (DE) is a function of the complex refractive index of the material pair, thickness t , the outermost zone width dr_N and so on, which are key structure parameters for FZP (Refs 6, 8–10). With the demanding of nanotechnology, FZP with small dr_N and high t is urgently required to obtain high resolution and DE of X-ray microscopy, especially for hard X-ray. While, the conventional e-beam lithography fabrication technique of X-ray FZP seems to be an immense challenge for achieving a small dr_N and larger t (Refs 11, 12). The FZP t could only restricted to 750–900 nm as the dr_N is 30–40 nm (Refs 13–17). In recent years, multilayer Fresnel zone plate (ML-FZP) has been proposed and shows an attractive prospect for preparation of FZPs with high aspect ratios. It comes from the sputter-sliced idea (Refs 18–21), coating alternative layers of suitable materials with precise zone width on a cylindrical substrate and then slicing an FZP with any desired high t from the deposited substrate. Several ML-FZPs fabricated by atomic layer deposition (ALD) and focused ion beam (FIB) have been reported. Al_2O_3/HfO_2 ML-FZP with dr_N 25 nm is fabricated through ALD and FIB slicing, the aspect ratio of which comes up to 500 with 12.6 μm thickness (Ref 21). Besides that, the aspect ratio of Al_2O_3/Ta_2O_5 ML-FZPs fabricated via ALD and FIB used at hard X-ray achieves 169 with dr_n 35 nm and thickness 5.9 μm (Refs 7, 19).

Typical numerical analytical methods for calculating FZP include finite-difference time domain (FDTD) (Refs 22–24), complex amplitude superposition theory (CAST) (Refs 25, 26) and coupled wave theory (CWT) (Refs 27–30). FDTD is a method that could obtain the global light intensity distribution; however, it is impractical to analyse the X-ray FZP due to its huge amount of computation and the dependence on computing equipment (Refs 26, 31, 32). CAST is a classical method provided by Kirz and has been widely used to calculate FZP DE (Refs 25, 33). Within the framework of CAST, FZP DE were usually calculated by the thin-grating approximation, and under the assumption of the outermost zone width is sufficiently large or the FZP thickness t is small to neglect dynamical diffraction effect which leads to the decrease of diffraction light intensity and diffraction, owing to the energy loss between wave vectors in different directions when X-rays pass through a grating with a smaller size (Refs 9, 25, 34), which

© The Author(s) 2024. Published by Cambridge University Press. This is an Open Access article, distributed under the terms of the Creative Commons Attribution licence (<http://creativecommons.org/licenses/by/4.0>), which permits unrestricted re-use, distribution and reproduction, provided the original article is properly cited.

is not suitable for ML-FZP with large thickness. CWT is an electromagnetic vector diffraction theory that preferred the energy exchanges between materials and photons through wave equations (Refs 27, 35). Traditionally, CWT is used to describe the coupling relationship between incident and diffracted lights through a periodic grating (Refs 27, 28). While, FZP is a non-periodic structure radially with the zone width decreasing gradually from inner to outside. It is assumed that these adjacent zones with slow changes of width are local periodic grating and then the *DE* of FZP has been estimated through CWT (Refs 29, 30). Whereas, the CWT *DE* calculations were just done for the outermost period dr_N locally (Ref 35), which is particularly inappropriate to represent *DE* of the whole FZP. This is owing to the zone widths in the FZP central region are apparently larger than the outside region and that will play a leading role in the focused energy. It is inaccurate to calculate the whole FZP *DE* simply using the outermost period dr_N locally.

In this work, theoretical *DEs* of ML-FZPs are firstly compared through CAST and CWT. Combining material pairs, all zone widths, dr_N , t and X-ray energy together, a partition calculation method (PCM) is proposed to design and evaluate FZP completely. The results obtained through PCM are validated by comparing them with the numerical results of CAST and CWT.

Comparison of CAST and CWT

FZP is a special kind of variable width grating (Fig. 1A), the FZP zone width dr_n is determined by Eq. (1) (Ref 25):

$$dr_n = \sqrt{n} \times r_1/2 \quad (1)$$

$$r_1 = \sqrt{\lambda f + \lambda^2/4} \quad (2)$$

where f , λ and r_1 are the focal length, X-ray wavelength and zone width of the first ring, respectively. This satisfies the FZP principle

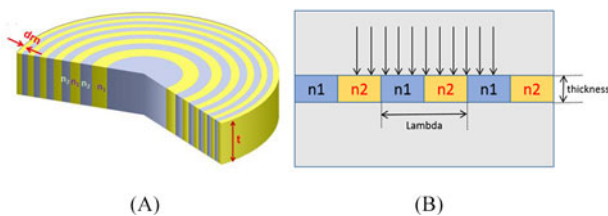


Figure 1. (A) Schematic structural diagram of FZP. (B) Local grating approximation.

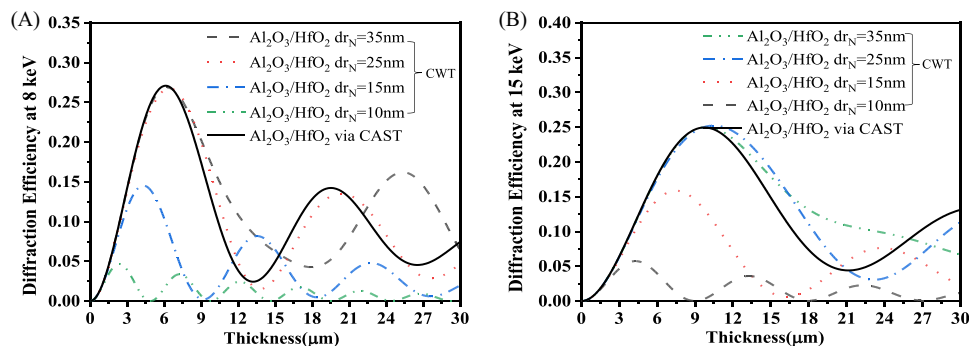


Figure 2. Theoretical ML-FZP *DEs* calculated by CAST and CWT with a decreasing dr_N for $\text{Al}_2\text{O}_3/\text{HfO}_2$ at (A) 8 keV and (B) 15 keV.

that the incident light passes through the adjacent half bands with different refractive indexes and then reaches the focal point with optical path differences of light wavelength λ and phase differences of 2π , which realizes the focusing at the focal point (Refs 35, 36).

The first-order *DE* is a key parameter as important as the resolution to evaluate FZP performance. According to CAST, the incident light passes through FZP and is focused according to the geometric relationship. There are some assumptions here that the zone width is sufficiently large or the FZP thickness t is extremely small, which can eliminate the need for consideration of the dynamic efficiency. Based on this, *DE* is calculated by comparing the superposed focus light intensity with incident light intensity as formula (3) (Ref 37):

$$DE = (1/\pi^2) \times \{ \exp(-2k\beta_1 t) + \exp(-2k\beta_2 t) - 2\exp[-k(\beta_1 + \beta_2)t] \times \cos[k(\delta_1 - \delta_2) \times t] \} \quad (3)$$

where $k = 2\pi/\lambda$, and the complex refractive index of the material is expressed as $n = 1 - \delta - \beta i$ which describes the absorption and attenuation of light as it passes through the material. It is shown that only the material refractive indexes and FZP t are considered in CAST.

CWT is an electromagnetic vector diffraction theory to calculate *DE* of periodic grating which combines Maxwell equations and boundary conditions to describe the coupling relationships between an incident and diffracted light (Refs 18, 25, 33, 34). According to Eq. (1) the local zone period $2dr_n$ changes slowly when zone number n is larger. Therefore, the FZP is approximated as an infinite periodic grating locally with a local period of $2dr_n$. Figure 1B shows the FZP approximate grating model, through which the FZP *DE* could be estimated locally by CWT (Refs 18, 19).

The differences of the absorption coefficients and phases for X-rays between Al_2O_3 and HfO_2 are large, leading to high *DEs* for X-rays with $\text{Al}_2\text{O}_3/\text{HfO}_2$ material pairs (Refs 21, 38). Moreover, these two materials have high melting points and stable chemical properties, which enable them in a large ALD common temperature growth interval (Ref 21). Thus $\text{Al}_2\text{O}_3/\text{HfO}_2$ is selected as the multilayer film material for numerical analysis. ML-FZP *DEs* calculated by CAST and CWT is compared in Fig. 2. In all situations, the *DE* oscillates periodically with ML-FZP thickness t . The CAST *DE* is mainly dependent on t at a given photon energy and material pairs. As Fig. 2A shows, the maximum CAST *DEs* are above 25% at 8 keV no matter how the zone widths are. Actually, when X-ray pass through a grating with a smaller size, plenty of energy is exchanged between wave vectors in different directions (Refs 23, 24), which leads to a decrease in diffraction light intensity and *DE*. While the *DE* calculated by CWT displays a sharp decrease as dr_N decreased below 25 nm. Take $\text{Al}_2\text{O}_3/\text{HfO}_2$ at 8 keV as an

example, the calculated maximum CAST *DE* is 27.6% at the optimum *t* 6.1 μm, and the maximum CWT *DE* decreases to 14.8% at *t* 4.5 μm and 4.9% at *t* 2.9 μm when *dr_N* reducing to 15 and 10 nm, respectively.

In addition, as shown in Fig. 2, we could obtain that the *DE* calculated by CWT is changed greatly with the zone width. Such a grating approximation method that only considers the *dr_N* is inappropriate and might cause great errors. The following two main reasons should be taken into account. Firstly, the central rings of FZP have larger zone widths (about >25 nm) and then higher *DE*, which should not be ignored. In addition, the *DE* descends greatly as the zone width decreases from 25 nm. We consider that the impact of all zones on *DE* should be calculated.

Furthermore, comparing Fig. 2A and B shows the optimal Al₂O₃/HfO₂ ML-FZP *t* is larger at 15 keV than at 8 keV for the same *dr_N* because of its strong penetrability in which thicker materials are needed to realize π phase shift. The optimal *t* increases from 4.5 and 2.9 μm to 8.7 and 5.1 μm when X-ray energy is raised from 8 to 15 keV at *dr_N* of 15 and 10 nm, respectively.

Given the above, in order to satisfy the application of X-ray microscopy imaging, all zone widths, thicknesses, X-ray energies and material pairs should be fully considered when calculating ML-FZP *DE*.

DE calculated by PCM

To calculate and analyse the FZP *DE* more reasonably and accurately, it is necessary to comprehensively consider the X-ray focusing and diffraction characteristics of all the zones, *dr_N*, *t* and material pairs of FZP. A PCM is proposed here. It derives as follows:

Generally, *DE* is defined as the ratio of the energy *E_{out_total}* of diffracted light to the total energy *E_{in_total}* of the incident light, and then:

$$E_{out_total} = \eta \times E_{in_total} \tag{4}$$

Assuming that the FZP zone number is *n*, the incident light energy of each zone is expressed as *E_{m(n)}* with its corresponding efficiency of *η_(n)*, then the diffracted X-ray energy can be expressed as follows:

$$E_{out_total} = (\eta_1 \times E_{in1} + \eta_2 \times E_{in2} + \dots + \eta_{n-1} \times E_{in(n-1)} + \eta_n \times E_{in(n)}) \tag{5}$$

The incident energy is defined as the total energy received by each zone of FZP. The area of each FZP zone is approximately equal based on the Fresnel criterion and the number of photons received per unit area is equal. It is reasonable to determine that the energy irradiated to the same area is equal, so the total energy of incident light can be expressed as follows:

$$E_{in_total} = n \times E_{in_zone} \tag{6}$$

The total *DE* of the FZP conforms to the following equation:

$$\eta = \frac{E_{out_total}}{E_{in_total}} = \frac{\eta_1 \times E_{in1} + \eta_2 \times E_{in2} + \dots + \eta_{n-1} \times E_{in(n-1)} + \eta_n \times E_{in(n)}}{n \times E_{in_zone}} \tag{7}$$

In the formula, the incident X-ray energy of the half band is equal, and the above formula can be rewritten as

$$\eta = \frac{\eta_1 + \eta_2 + \dots + \eta_{n-1} + \eta_n}{n} \tag{8}$$

Therefore, the FZP *DE* can be expressed by the average value of each zone *DE* as formula (8). Since the FZP zone number is generally large, such as 6200 rings for Al₂O₃/HfO₂ ML-FZP with *dr_N* 10 nm, diameter 0.25 mm, in order to improve the calculation efficiency, we can divide the FZP into several regions according to the fluctuation degree of the *DE*. Two principles are used here for the segmentation: first, the *DE* fluctuation in a region is not greater than 1%; second, the average *DE* fluctuation is not exceeding 1000th, where (the average *DE* fluctuation) = [*DE* fluctuation × (zone number in this region)]/(total zone number). By this time, the *DE* could be assumed nearly equal in each region. Then, according to the characteristics of different regions, the CAST or CWT method is reasonably selected to calculate the *DE* for specific region. For regions with large *dr_n* near the centre, CAST can be used; with *dr_n* decreasing along the radial direction, CAST is no longer applicable, and CWT can play an advantage at this time. What follows is weighted averaging of the *DE* of all regions and obtaining the ML-FZP *DE* as reasonably and accurately as possible.

Taking Al₂O₃/HfO₂ ML-FZP with *dr_N* of 10 nm and focal length of 16 mm as an example, the total zone numbers are 6200, of which 3444 rings have a zone width 10–15 nm, 1206 rings lie in 15–20 nm,

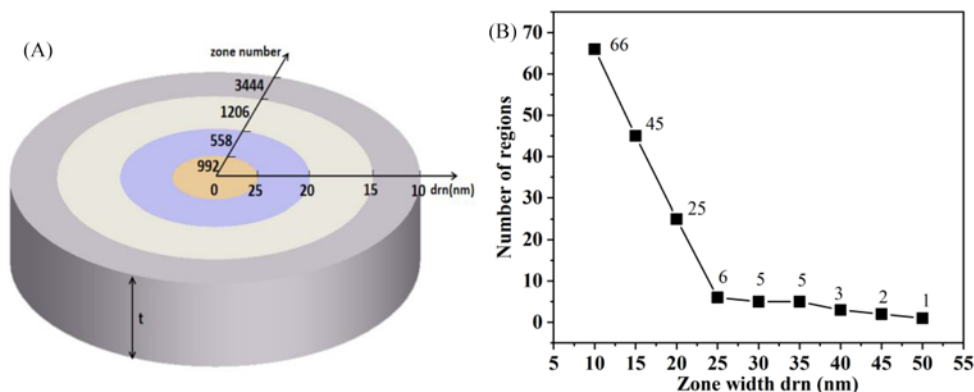


Figure 3. (A) Schematic diagram of the zone number and (r) region number calculated by PCM in different zone width intervals for Al₂O₃/HfO₂ ML-FZP with X-ray energy, *dr_N* and focal length *f* are 8 keV, 10 nm and 16 mm, respectively.

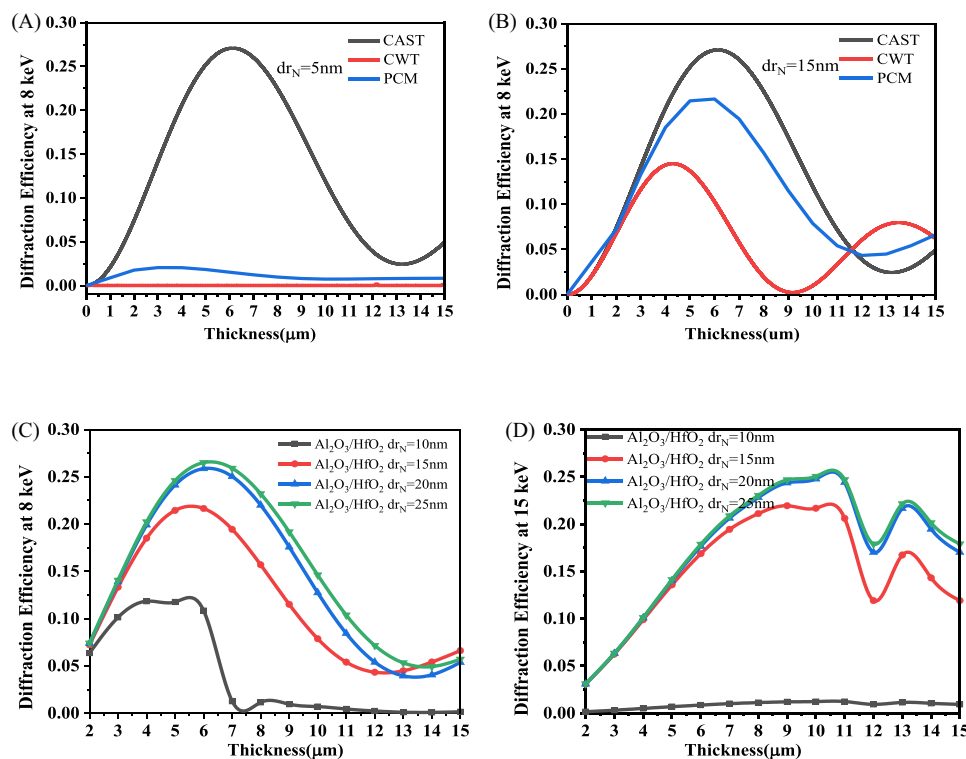


Figure 4. $\text{Al}_2\text{O}_3/\text{HfO}_2$ ML-FZP DEs compared by CAST, CWT and PCM vs FZP t at 8 keV with (A) dr_N 5 nm, (B) dr_N 15 nm; DEs calculated by the proposed PCM vs FZP t with dr_N 10, 15, 20 and 25 nm, respectively at (C) 8 keV and (D) 15 keV.

558 rings lie in 20–25 nm and 992 rings have the zone width larger than 25 nm, as Fig. 3A is shown. Based on PCM, the $\text{Al}_2\text{O}_3/\text{HfO}_2$ ML-FZP in Fig. 3A is divided into 158 regions as shown in Fig. 3B. It can be found that the region number increases linearly as dr_N decreases from 25 to 5 nm and fewer regions is required with dr_N above 25 nm, which depended closely on the DE fluctuation.

For outer rings with larger n , as the zone widths changed slowly, the FZP DE could be approximately calculated as a periodic grating with $2dr_N$ as a period through CWT (Refs 19, 39). That is, the ML-FZP DE is calculated here as an infinite periodic grating with a half-period of 10 nm.

As an illustration, $\text{Al}_2\text{O}_3/\text{HfO}_2$ ML-FZP DEs evaluated by CAST, CWT and PCM are compared in Fig. 4A for dr_N 5 nm and in Fig. 4B for dr_N 15 nm. It can be seen that the largest DE is estimated through CAST because the energy attenuation caused by the dynamic effect is ignored. Meanwhile, it is more undesirable to just consider the dr_N and based on this period to estimate the CWT DE of infinite periodic grating as that of the whole FZP, which causes the DE to be too low. The proposed PCM consideration of the focusing performance of all the FZP zones, which provides a reasonable way to calculate DE as accurately as possible.

Moreover, the $\text{Al}_2\text{O}_3/\text{HfO}_2$ ML-FZP DE curves with dr_N 10, 15, 20 and 25 nm at 8 and 15 keV are also calculated via PCM as shown in Fig. 4C and D, from which the theoretical maximum DE and optimal t could be estimated. It can be seen that, due to dynamic diffraction effects, the decrease of dr_N below a certain threshold makes an obvious influence on the ML-FZP DE significantly, especially at high energy. Besides, a higher t is desired at larger energy to achieve maximum DE of ML-FZP. For ML-FZP with extra small dr_N , such as 10 nm, $\text{Al}_2\text{O}_3/\text{HfO}_2$ ML-FZP has a maximum theoretical DE of 12.3% at 8 keV with t 4–6 μm , while as the X-ray energy

increase to 15 keV, corresponding DE is below 1%, which indicates the material pair is selective for energy applied in X-ray imaging. In addition, the DE curves display multiple peaks at 15 keV which mainly depended on the complex relationship between the FZP structures, material pairs and X-ray.

From the results above, it can be seen that as the FZP aspect ratio increases, more factors and parameters should be considered, which have a great impact on the DE. CAST is a method that calculates FZP DE without reflecting on the zone width, while CWT evaluates DE using the outermost zone width dr_N only. Combining all zone widths, t , material pair and X-ray energy, the PCM is seriously proposed to estimate the FZP DE more exactly. It is of great significance for the design and fabricating of FZP with high DE and resolution, especially for the resolution below 25 nm.

Conclusion

This work investigates the DE numerical analysis method of X-ray ML-FZP with high aspect ratios. Firstly, DEs of ML-FZPs are estimated through CAST and CWT. Based on geometrical optics theory, CAST does not consider the dynamic diffraction attenuation of the FZP although that increases with the decrease of dr_N . In addition, the numerical results of CWT show that the FZP DE varies greatly with the width of zones. In order to meet the requirements of higher imaging resolution and DE, large FZP diameter and small dr_N that induced the differences between the centre and outer zones increasing are necessary. Thus, CWT which approximates the FZP as a periodic thin grating is also no longer applicable.

Based on the results above, an approach PCM that considers the focusing performances of all zones is proposed to calculate FZP DE

more completely. In the way, FZP is divided into several regions according to the *DE* fluctuation. Appropriate numerical analysis method is selected according to the property of each region and then averaging weighted *DEs* of all regions receive the FZP *DE*. As a validation example, the $\text{Al}_2\text{O}_3/\text{HfO}_2$ ML-FZP with dr_N 10 nm and 6200 rings could be divided into 158 regions that calculated a maximum *DE* of 12.3% at 5.6 μm by PCM, significantly reducing the amount of computation. The results obtained through PCM are validated by comparing them with CAST and CWT numerical results. It is extremely meaningful for designing and evaluating FZP more accurately. Combining proper numerical analysis with the experimental conditions will present a great potential to break through the imaging performance of X-ray microscopy.

Financial Support. This work was supported in part by the National Key Research and Development Program of China (Grant No. 2018YFA0704804), Chinese Academy of Sciences Scientific Instrument and Equipment Development Project (Grant No. ZDKYYQ20220001), Frontier Project of the Northern Advanced Technology Research Institute (Grant No. QYJS-2022-1800) and Beijing Municipal Science and Technology Plan (Grant No. Z231100006623011).

Conflicts of Interest. Authors declare no conflicts of interest.

References

- Shuyue C, and Hongnian L (1999) Research and development of digital X-ray radiography in nondestructive testing. *Journal of North China Institute of Science and Technology* **20**, 51–55.
- Myneni SCB (2002) Soft X-ray spectroscopy and spectromicroscopy studies of organic molecules in the environment. *Reviews in Mineralogy and Geochemistry* **49**, 485–579.
- Sakdinawat A and Attwood D (2010) Nanoscale X-ray imaging. *Nature Photonics* **4**, 840–848.
- Kodur M, Kumar RE, Luo YQ, Canak DN, Li XY, Stuckelberger M and Fenning DP (2020) X-ray microscopy of halide perovskites: Techniques, applications, and prospects. *Advanced Energy Materials* **10**, 1903170.
- Jie MA, Lei-feng CAO, Chang-qing XIE, Xuan WU, Hai-liang LI, Xiao-li ZHU, Ming LIU, Bao-qin C and Tian-chun YE (2009) Fabrication of high aspect-ratio hard X-ray zone plates with supporting structures. *Opto-Electronic Engineering* **36**, 30–34.
- Zhang BZ (2010) Design of zone plates and their diffraction characteristics, Ph.D. Zhejiang University.
- Keskinbora K, Robisch AL, Mayer M, Sanli UT, Grevent C, Weigand M, Szeghalmi A, Knez M, Salditt T and Schutz G (2014) Multilayer Fresnel zone plates for high energy radiation resolve 21 nm features at 1.2 keV. *Optics Express* **22**, 18440–18453.
- Tong XJ, Chen YF, Mu CY, Chen QC, Zhang XZ, Zeng G, Li YC, Xu ZJ, Zhao J, Zhen XJ, Mao CW, Lu HL and Tai RZ (2023) A compound Kinoform/Fresnel zone plate lens with 15 nm resolution and high efficiency in soft x-ray. *Nanotechnology* **34**, 215301.
- Pommet DA, Moharam MG and Grann EB (1994) Limits of scalar diffraction theory for diffractive phase elements. *Journal of the Optical Society of America A-Optics Image Science and Vision* **11**, 1827–1834.
- Li KN, Ali S, Wojcik M, de Andrade V, Huang XJ, Yan HF, Chu YS, Nazaretski E, Pattammattel A and Jacobsen C (2020) Tunable hard x-ray nanofocusing with Fresnel zone plates fabricated using deep etching. *Optica* **7**, 410–416.
- Gorelick S, Vila-Comamala J, Guzenko VA, Barrett R, Salome M and David C (2011) High-efficiency Fresnel zone plates for hard X-rays by 100 keV e-beam lithography and electroplating. *Journal of Synchrotron Radiation* **18**, 442–446.
- Chen YT, Lo TN, Chiu CW, Wang JY, Wang CL, Liu CJ, Wu SR, Jeng ST, Yang CC, Shiu J, Chen CH, Hwu Y, Yin GC, Lin HM, Je JH and Margaritondo G (2008) Fabrication of high-aspect-ratio Fresnel zone plates by e-beam lithography and electroplating. *Journal of Synchrotron Radiation* **15**, 170–175.
- Chao W, Kim J, Rekawa S, Fischer P and Anderson EH (2009) Demonstration of 12 nm resolution Fresnel zone plate lens based soft X-ray microscopy. *Optics Express* **17**, 17669–17677.
- Divan R, Mancini DC, Moldovan N, Lai B, Assoufid L, Leonard Q and Cerrina F (2002) Progress in the fabrication of high-aspect-ratio zone plates by soft x-ray lithography. In Conference on Design and Microfabrication of Novel X-Ray Optics, Proceedings of SPIE 2002), 82–91.
- Liu JB, Shao JH, Zhang SC, Ma YQ, Taksatorn N, Mao CW, Chen YF, Deng BA and Xiao TQ (2015) Simulation and experimental study of aspect ratio limitation in Fresnel zone plates for hard-x-ray optics. *Applied Optics* **54**, 9630–9636.
- Liu LH, Xiong Y, Chen J, Li WJ and Tian YC (2010) Fabrication of X-ray imaging zone plates by e-beam and X-ray lithography. *Microsystem Technologies-Micro-and Nanosystems-Information Storage and Processing Systems* **16**, 1315–1321.
- Zhu JY, Zhang SC, Xie SS, Xu C, Zhang LJ, Tao XL, Ren YQ, Wang YD, Deng B, Tai RZ and Chen YF (2020) Nanofabrication of 50 nm zone plates through e-beam lithography with local proximity effect correction for x-ray imaging. *Chinese Physics B* **29**, 047501.
- Takano H, Sumida K, Hiroto H, Koyama T, Ichimaru S, Ohchi T, Takenaka H and Kagoshima Y (2016) Hard X-ray multilayer zone plate with 25-nm outermost zone width. In 13th International X-Ray Microscopy Conference (XRM), Journal of Physics Conference Series 2016), 012052.
- Mayer M, Keskinbora K, Grevent C, Szeghalmi A, Knez M, Weigand M, Snigirev A, Snigireva I and Schutz G (2013) Efficient focusing of 8 keV X-rays with multilayer Fresnel zone plates fabricated by atomic layer deposition and focused ion beam milling. *Journal of Synchrotron Radiation* **20**, 433–440.
- Li YL, Lu WE, Wang SF, Yuan QX, Kong XD, Han L and Xia Y (2023) Fabrication of multilayer Fresnel zone plate for hard X-ray microscopy by atomic layer deposition and focused ion beam milling. *Vacuum* **209**, 111776.
- Sanli UT, Jiao C, Baluksian M, Grevent C, Hahn K, Wang Y, Srot V, Richter G, Bykova I, Weigand M, Schutz G and Keskinbora K (2018) 3D nanofabrication of high-resolution multilayer Fresnel zone plates. *Advanced Science* **5**, 1800346.
- Lee KY, Shyu MH, Huang JB, Jeng SS, Juinn-Shien L and Lin YJ (2006) Scalar FDTD analysis of Fresnel zone-plate lenses. *Journal of Optical Communications* **27**, 11–13.
- Toroglu G and Sevgi L (2014) Finite-difference time-domain (FDTD) MATLAB codes for first-and second-order EM differential equations. *IEEE Antennas and Propagation Magazine* **56**, 221–239.
- Luebbers RJ, Kunz KS, Schneider M and Hunsberger F (1991) A finite-difference time-domain near zone to far zone transformation. *IEEE Transactions on Antennas and Propagation* **39**, 429–433.
- Kirz J (1974) Phase zone plates for X-rays and extreme UV. *Journal of the Optical Society of America* **64**, 301–309.
- Xiao K (2006) Research on Soft X-ray Condenser Zone Plates, Ph.D. University of Science and Technology of China.
- Zhang N, Chu J, Zhao K and Meng F (2006) The design of the subwavelength wire-grid polarizers based on rigorous couple-wave theory. *Chinese Journal of Sensors and Actuators* **19**, 1739–1743.
- Liu Q and Wu J (2004) Analysis and comparison of the scalar diffraction theory and coupled-wave theory about grating. *Laser Journal* **25**, 31–33.
- Zhu Y, Zhang Y and Zhao Y (2014) Vertical diffraction of multi-step hybrid Fresnel zone plates. *Laser & Optoelectronics Progress* **51**, 60501.
- Batterman BW and Cole H (1964) Dynamical diffraction of X rays by perfect crystals. *Reviews of Modern Physics* **36**, 681–8.
- Mirotznik MS, Prather DW, Mait JN, Beck WA, Shi SY and Gao X (2000) Three-dimensional analysis of subwavelength diffractive optical elements with the finite-difference time-domain method. *Applied Optics* **39**, 2871–2880.

32. **Prather DW, Shi SY and Sonstroem J** (2002) Electromagnetic analysis of finite-thickness diffractive elements. *Optical Engineering* **41**, 1792–1796.
33. **Kirz J, Jacobsen C and Howells M** (1995) Soft-X-ray microscopes and their biological applications. *Quarterly Reviews of Biophysics* **28**, 33–130.
34. **Yun WB, Viccaro PJ, Lai B and Chrzas J** (1992) Coherent hard x-ray focusing optics and applications. *Review of Scientific Instruments* **63**, 582–585.
35. **Maser J** (1992) Evaluation of the efficiency of zone plates with high aspect ratios by application of coupled wave theory. In *X-Ray Microscopy III: Proceedings of the Third International Conference*, London, September 3–7, 1990, Springer, 104–106.
36. **Rehbein S, Heim S, Guttman P, Werner S and Schneider G** (2009) Ultrahigh-resolution soft-X-ray microscopy with zone plates in high orders of diffraction. *Physical Review Letters* **103**, 110801.
37. **Wang S** (2019) Fabrication of X-ray zone plates with large aspect ratio. Master, Beijing Jiaotong University.
38. **Sanli UT, Keskinbora K, Leister J, Teeny N, Grévent C, Knez M and Schütz G** (2015) High resolution, high efficiency multilayer Fresnel zone plates for soft and hard X-rays. In *Conference on X-Ray Nanoimaging - Instruments and Methods II*, Proceedings of SPIE 2015.
39. **Gao Y, Wu L, Lu W, Liu H, Xia Y, Zhao L, Li Y, Kong X and Han L** (2021) Design of hard X-ray Fresnel zone plates based on rigorous coupled wave theory. *Acta Optica Sinica* **41**, 1111002.